SCIENTIFIC REPORTS

OPEN

SUBJECT AREAS:
CATALYST SYNTHESIS
POLLUTION REMEDIATION
HETEROGENEOUS CATALYSIS
POLLUTION REMEDIATION

Received
21 January 2015

Accepted
17 March 2015

Published
19 May 2015

Correspondence and requests for materials should be addressed to R.W. (ruihu@fjirsm.ac.cn)

Bauxite-supported Transition Metal Oxides: Promising Low-temperature and SO_2-tolerant Catalysts for Selective Catalytic Reduction of NO_x

Xiuyun Wang[1,2], Wen Wu[1,2], Zhilin Chen[1] & Ruihu Wang[1,2]

[1]State Key Laboratory of Structural Chemistry, Fujian Institute of Research on the Structure of Matter, Chinese Academy of Sciences, Fuzhou, Fujian, 350002, China.Tel:86-591-83711028; Fax:86-591-83714946, [2]Key Laboratory of Coal to Ethylene Glycol and Its Related Technology, Chinese Academy of Sciences, Fuzhou 350002, China.

In order to develop low-temperature (below 200 °C) and SO_2-tolerant catalysts for selective catalytic reduction (SCR) of NO_x, a series of cheap M/bauxite (M = Mn, Ni and Cu) catalysts were prepared using bauxite as a support. Their SCR performances are much superior to typical V_2O_5/TiO_2, the addition of M into bauxite results in significant promotion of NO_x removal efficiency, especially at low temperature. Among the catalysts, Cu/bauxite exhibits wide temperature window over 50–400 °C, strong resistance against SO_2 and H_2O as well as good regeneration ability in SCR of NO_x. NO_x conversion is more than 80% at 50–200 °C, and N_2 selectivity is more than 98%. Cu/bauxite can serve as a promising catalyst in SCR of NO_x.

Nitrogen oxides (NO_x) are considered as one of serious air pollutants, they are mainly emitted from automobile exhaust gas and industrial combustion of fossil fuels.[1–3] To meet for more and more stringent regulations of NO_x emission, several promising techniques including NO_x storage and reduction (NSR) and selective catalytic reduction (SCR) have been proposed for NO_x post-treatment.[2,3] Among these techniques, SCR of NO_x with NH_3 is an efficient process to remove NO_x from diesel vehicles and stationary sources.[4–9] Titania-supported vanadia with WO_3 or MoO_3 as promoters are typical commercial catalysts for SCR of NO_x.[8–10] Nevertheless, these catalysts usually suffer from some problems, such as toxicity of vanadium, SO_2 oxidation to SO_3, over-oxidation of NH_3 to N_2O, and employment within a high and narrow temperature window of 300–400 °C.[11] Due to their high operating temperature, the catalysts are always located at upstream of purification system and/or desulfurization units, resulting in deactivation in the presence of high concentrations of dust and SO_2.[12,13] Thus, the development of SO_2-tolerant SCR catalysts working below 200 °C has attracted considerable attention.

Noble metal-based catalysts are well known to possess good catalytic activity and high selectivity in low-temperature SCR of NO_x,[14] but high price and scarcity of noble metal source have limited their extensive application and further development. Several groups of metal oxide-based catalysts have been reported to possess the advantages of low cost, high thermal stability and good activity for NO_x reduction,[15] further improvement of overall SCR performances has also been realized through the judicial combinations of different metal oxides with potential catalytic activity.[15,16] Although the mixed transition metal oxides show high SCR activity below 200 °C, their catalytic activity rapidly decreases in the presence of SO_2.

It is proposed that SCR performances, sulfur tolerance and thermal stability of catalysts may be adjusted through formulation modification, structure adjustment and use of complicate supports.[17,18] In the context, multi-metal oxides are widely used as the supports of SCR catalysts since they can provide superior general properties through synergetic interactions of their compositions.[18–20] Bauxite is composed of Al_2O_3, FeO_x, TiO_2, SiO_2 and trace of Pt, these compositions are well known to be advantageous in NO_x removal.[21] In addition, natural bauxite is cheap, readily available and non-toxic, long period of natural evolution may offer it good stability. In our continuous effort to develop highly efficient and SO_2-tolerant SCR catalysts,[22,23] herein, we report a series of bauxite-supported transition metal oxides, M/bauxite (M = Mn, Ni and Cu), they show superior SCR performances over typical V_2O_5/TiO_2. NO_x conversion in Cu/Bauxite is more than 80% in 50–200 °C, moreover,

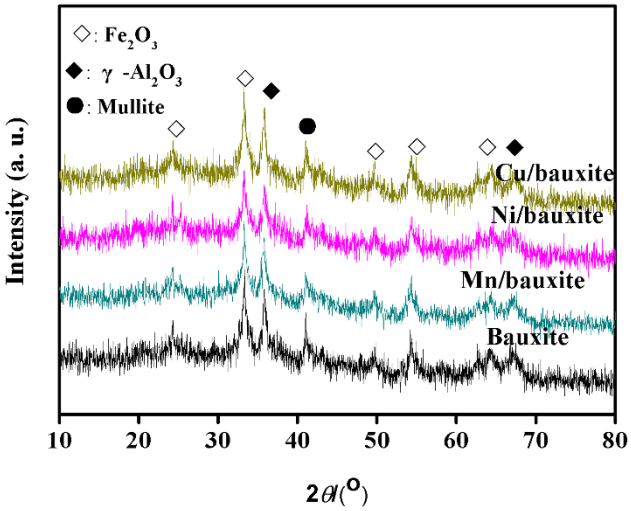

Figure 1 | **XRD patterns of bauxite and M/bauxite.**

Cu/bauxite shows high N_2 selectively, strong resistance against SO_2 and H_2O as well as good regeneration ability in SCR of NO_x.

Results

X-ray diffraction (XRD) pattern shows that bauxite possesses the characteristic peaks of crystalline γ-Al_2O_3 (JCPDS No. 44-1487), Fe_2O_3 (JCPDS No. 06-0502) and mullite phase (Figure 1), X-ray Fluorescence (XRF) and Inductively Coupled Plasma (ICP) analyses show the main compositions in the modified bauxite are Al_2O_3, Fe_2O_3, and SiO_2 (Table S2), which are and accordance with those from XRD patterns. After the addition of 3 wt% transition metal oxides, the surface area is decreased from 194 m^2/g to 130–138 m^2/g owing to the filling or blocking of partial pore. No phases of transition metal oxides are observed, suggesting that metal oxide species are finely dispersed on bauxite or they are too small to be detected by XRD analysis.

The surface valence state and concentration of M in M/bauxite were investigated by X-ray photoelectron spectroscopy (XPS) analysis. As shown in Figure 2, the binding energy peak of Cu $2p_{3/2}$ at 934.1 eV and the shake-up satellite at 942.7 eV reveal Cu^{2+} are the predominant species in fresh Cu/bauxite. XPS spectrum of Ni $2p_{3/2}$ indicates that Ni^{2+} (856.2 eV) is major phase in fresh Ni/bauxite,[18] while XPS spectrum of Mn $2p_{3/2}$ indicates that MnO_2 (642.2 eV) and Mn_2O_3 (641.2 eV) are major phases along with the third phase (643.8 eV), which is attributed to incomplete decomposition of Mn nitrate owing to relatively low calcination temperature.[18] As shown in Table S1, Cu/bauxite has the highest surface concentration of MO_x species (1.86 mol%), which means that more CuO_x species are available to participate in SCR of NO_x. The surface ratio of NiO_x in Ni/bauxite and MnO_x species in Mn/bauxite are 1.72 and 1.15 mol%, respectively, regardless of the same loading in the preparation of the catalysts.

SCR performances of M/bauxite were initially evaluated using NH_3 storage capacity and NO_x conversion.[13] As shown in Table S3, the storage capacities at 50 ℃ in Mn/bauxite, Ni/bauxite and Cu/bauxite are 0.66, 0.69 and 0.84 mmol/g, which are much higher than 0.30 mmol/g in V_2O_5/TiO_2. As the temperature is elevated, their storage capacities are gradually lowered. As expected, bauxite itself possesses catalytic activity in SCR of NO_x with NH_3. NO_x conversion is over 40% at 50–200 ℃, which is slightly higher than that of V_2O_5/TiO_2 (Figure 3). The superior activity in bauxite probably results from the presence of FeO_x and trace amount of Pt. The addition of Mn, Ni and Cu leads to significant improvement of NO_x conversion, especially for Cu/bauxite, which is mainly attributed to the promotion effect of MO_x species in the oxidation of NO to NO_2, since NO_2 is more reactive than NO in SCR. More than 80% of NO_x conversion at 50–200 ℃ can be achieved in Cu/bauxite, which almost reaches two times of that in bauxite and V_2O_5/TiO_2. When temperature is increased above 200 ℃, the reduction ability of NO_x in Cu/bauxite and Ni/bauxite is close to each other, their NO_x conversion almost reaches 90% at 200 ℃, and is more than 98% after 250 ℃. For V_2O_5/TiO_2, NO_x conversion begins to quickly increase after 200 ℃, NO_x conversion at 300–400 ℃ is more than 96%, which is close to

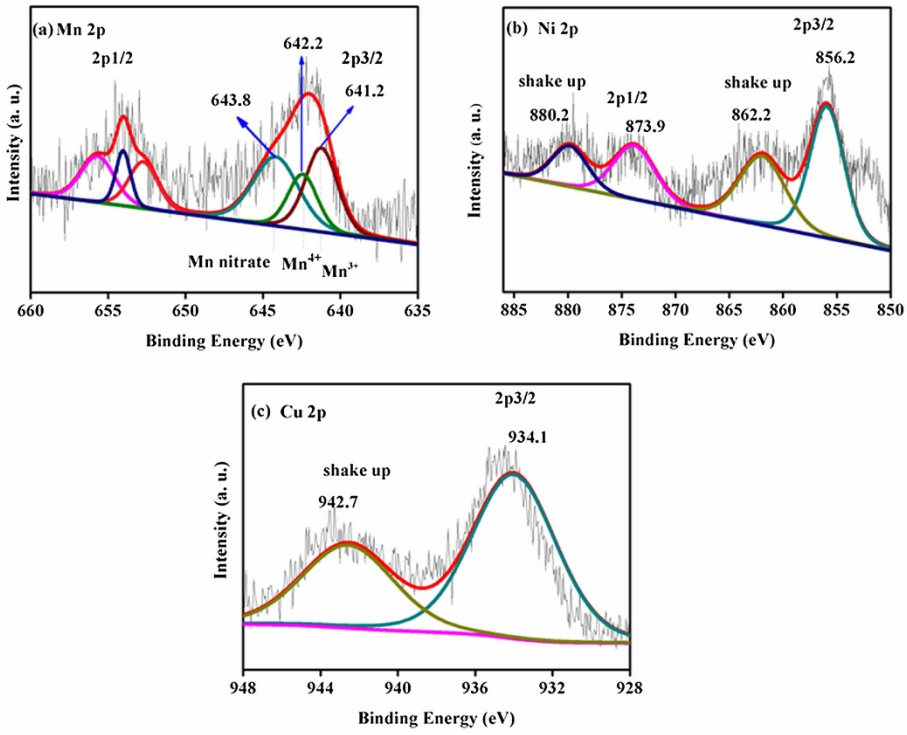

Figure 2 | **XPS spectra for Mn 2p, Ni 2p and Cu 2p.**

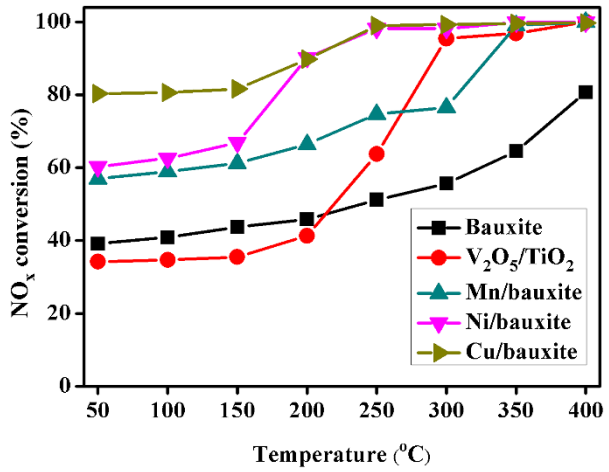

Figure 3 | NO_x conversion of M/bauxite and V_2O_5/TiO_2 at different temperatures.

that in Cu/bauxite and Ni/bauxite. Interestingly, the light-off temperature (the temperature where NO_x conversion reaches 50%, T_{50}) is found to be less than 50 ℃ in M/bauxite, while it is around 250 ℃ in V_2O_5/TiO_2. SCR activity of Cu/bauxite is also compared with that of the reported Cu/zeolite or Fe/zeolite,[13] higher NO_x conversion at low-temperature and wider temperature window are shown in Cu/bauxite. The superior SCR performances in Cu/bauxite encouraged us to further investigate its selectivity. As shown in Figure S1, N_2 selectivity maintains about 98% in 50–400 ℃, while selectivity of N_2O is less than 2%.

The effect of inlet NO_2/NO_x ratio on SCR activity was also investigated in Cu/bauxite. As shown in Figure S2, NO_x conversion of Cu/bauxite is gradually enhanced when NO_2/NO_x ratio is increased from 0.25 to 0.5, and reaches the maximum at 0.5, subsequent drop of NO_x conversion is observed at 0.75 and 1.0. It was reported that when NH_3 and NO_2 were fed into the reactor, NH_4NO_3 can be formed at low temperature.[1,13] Since NH_4NO_3 cannot be detected directly by our apparatus, transient response method (TRM) of Cu/bauxite at 150 ℃ was conducted to indirectly estimate the amount of NH_4NO_3 according to N-balance. As shown in Figure S3, when 500 ppm NH_3 and NO_2 were introduced into the systems, the formed N_2 and N_2O are 321 and 6 ppm, respectively. After the system reaches a steady state, the outlet ($NO+NO_2$) and NH_3 concentrations are 61 and 121 ppm, respectively. The lack of 165 ppm in the total amount of N evidences the formation of 82.5 ppm NH_4NO_3 in Cu/bauxite.

As the exhaust gas usually contains a trace amount of SO_2 (30–2000 ppm) and a large amount of H_2O (2–15 vol%),[15] the improvement of SO_2 and H_2O tolerance is one of the challenges for NH_3-SCR catalysts. NO_x conversions of Cu/bauxite and V_2O_5/TiO_2 were tested in a feed gas containing 100 ppm SO_2 at 200 and 350 ℃, respectively. As shown in Figure 4a, the presence of SO_2 results in quick decrement of NO_x conversion from 41 to 10% in V_2O_5/TiO_2 and from 89 to 40% in Cu/bauxite at 200 ℃. SO_2 tolerance of Cu/bauxite and V_2O_5/TiO_2 was further examined at 350 ℃ owing to similarity of their NO_x conversion at the temperature. As shown in Figure 4b, NO_x conversion in V_2O_5/TiO_2 decreases from 95% to below 40% at 350 ℃ in the presence of SO_2, while it is slightly lowered to 90% in Cu/bauxite under the same conditions. The superior tolerance toward SO_2 in Cu/bauxite probably results from the presence of FeO_x and TiO_2 in bauxite, which may inhibit the formation of sulfates and promote the decomposition of sulfates.[3] After the supply of SO_2 was cut off, and the sulfated catalysts were regenerated by 3.5 vol% H_2, NO_x conversion in Cu/bauxite and V_2O_5/TiO_2 is gradually restored, suggesting both Cu/bauxite and V_2O_5/TiO_2 possess good regeneration ability after SO_2 poisoning, but Cu/bauxite is highly sulfur-resistant. NO_x conversion was also examined in a feed gas containing 10 vol% H_2O at 200 ℃. The presence of H_2O results in a quick decrement of NO_x conversion from 89 to 75% in Cu/bauxite (Figure S4). After cutting off the supply of H_2O, NO_x conversion is rapidly restored to 89% at 200 ℃.

In order to clarify correlation between redox properties and SCR activities, bauxite and M/bauxite were characterized by H_2 temperature-programmed reduction (H_2-TPR). As shown in Figure S5, bauxite presents two broad reduction peaks similar to Fe_2O_3.[24] The peak at 420 ℃ corresponds to the reduction of Fe_2O_3 to Fe_3O_4, and the other peak at 683 ℃ is assigned as the reduction of Fe_3O_4 to FeO and subsequent reduction to Fe, suggesting FeO_x is main active component of NO_x reduction in bauxite. In M/bauxite, the two reduction peaks shift to lower temperatures, especially for the peak at 420 ℃, and they are in the following order: Cu/bauxite (326 ℃) < Ni/bauxite (385 ℃) < Mn/bauxite (392 ℃). The shift of the reduction peaks and difference in the peak area between bauxite and M/bauxite are ascribed to synergetic effect between bauxite and M. The synergetic effect through electron transfer between M and Fe ions maintains a dynamic equilibrium, and enhances the activity of low-temperature SCR in M/bauxite. For example, Fe^{3+} can capture an electron from Mn^{3+}, and they become Fe^{2+} and Mn^{4+} by the electron transfer. The formation of Fe^{2+} is responsible for changing NH_3 to $-NH_2$. The generated Fe^{2+} will reduce O_2 into O^{2-} by donating an electron to O_2, and simultaneously changes back to Fe^{3+} *via* $2Fe^{2+} + 1/2\ O_2 \leftrightarrow 2Fe^{3+} + O^{2-}$.

It should be mentioned that Cu/bauxite has two additional reduction peaks at 126 and 195 ℃, which may be attributed to the reduction of surface and bulk Cu^{2+} to Cu^+, respectively. The peak at 270 ℃ in Ni/bauxite can be assigned as the reduction of NiO_x, while no obvious reductive peak is observed in Mn/bauxite, because the reduction peak of MnO_2/Mn_2O_3 to MnO (300–400 ℃) is overlapped with that of Fe_2O_3 to Fe_3O_4. The reduction temperature of M in Cu/bauxite is much lower than that in Ni/bauxite and Mn/bauxite,

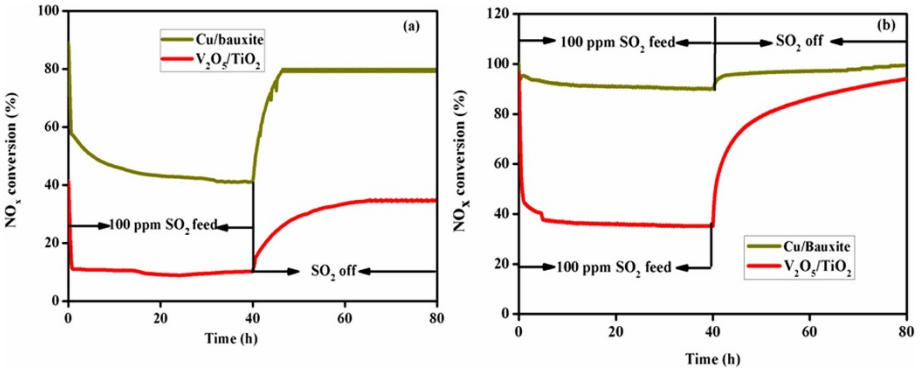

Figure 4 | SO_2-tolerance and regenerability of Cu/bauxite and V_2O_5/TiO_2 at 200 °C (a) and 350 °C (b) as function of time.

which is responsible for excellent low-temperature SCR activity in Cu/bauxite.

The adsorption behavior of catalysts is known to substantially affect SCR performances of NO_x.[25] NO_x temperature-programmed desorption (NO_x-TPD) experiments were carried out in order to determine the adsorption capacity of NO_x in bauxite and M/bauxite. As shown in Figure S6, two NO_x desorption peaks at 153 and 345 ℃ are observed in bauxite, which are assigned to desorption of NO_x and decomposition of surface adsorbed nitrite/nitrate species, respectively.[26] It is noteworthy that a strong desorption peak of NO_2 is also observed in bauxite, suggesting that bauxite is able to oxidize NO, which would be beneficial for SCR at low temperature.[12,13] The addition of Cu and Ni results in the increment of desorption temperature below 200 ℃ to 183 and 188 ℃, respectively, while the desorption temperature of NO_x in Mn/bauxite is decreased to 90 ℃ owing to weak interaction of NO_x with small MnO_2/Mn_2O_3 particles.[27] Interestingly, the peak intensity in M/bauxite is greatly increased in comparison with that of bauxite, suggesting that Mn, Ni and Cu addition is favorable for NO_x adsorption at low temperature. The desorption amounts of NO_x are in the order: Cu/bauxite > Ni/bauxite > Mn/bauxite > bauxite (Table S1), and this trend is in good agreement with their SCR activity. However, the relative area of desorption peak above 300 ℃ is decreased in M/bauxite in comparison with that of bauxite, especially for Cu/bauxite and Ni/bauxite. In addition, Mn addition results in a decrement of desorption temperature from 345 to 291 ℃, while Cu and Ni addition has no obvious effect on desorption temperature above 300 ℃.

It is well known that surface acidity plays an important role in low-temperature SCR of NO_x.[9] NH_3 temperature-programmed desorption (NH_3-TPD) was performed to investigate the type, amount and strength of surface acid. As shown in Figure S7, the shapes of NH_3 desorption profiles in M/bauxite are very similar to that in bauxite, in which two distinct desorption processes are presented. NH_3 desorption peak at low temperature contains a shoulder peak at 250–400 ℃. Obviously, the addition of Cu, Ni and Mn has no significant effect on desorption temperature below 200 ℃. However, NH_3 desorption amounts in Cu/bauxite and Ni/bauxite are almost similar to each other at low temperature, they are much larger than that in bauxite and Mn/bauxite (Table S1). The other desorption temperature above 500 ℃ in M/bauxite is higher than that in bauxite. Because NH_3 bound to Lewis acid sites is more thermally stable than NH_4^+ ions coordinated to Brønsted acid sites, the desorption peak at low temperature is mostly assigned to NH_4^+ ions on Brønsted acid sites, while the desorption peak at high temperature is associated with the adsorbed NH_3 on Lewis acid sites.[28–30] In comparison with bauxite, the addition of M has no obvious effect on strength of Brønsted acid sites, but it causes an obvious increment of strength of Lewis acid sites in M/bauxite. Obviously, larger Brønsted acid amount and stronger Lewis acid strength in Cu/bauxite and Ni/bauxite are favorable for facilitating adsorption and activation of NH_3 in SCR of NO_x.

in situ diffuse reflectance infrared Fourier transform spectroscopy (DRIFTS) of NH_3 adsorption was investigated to better understand properties of acid sites in bauxite and M/bauxite. As shown in Figure 5, with the increment of temperature, the peaks gradually become weak and almost disappear above 300 ℃, which is probably ascribed to unstability of the adsorbed NH_3 at high temperature. As for bauxite, two bands at 1245 and 1628 cm^{-1} are assigned to symmetric bending vibrations of the coordinated NH_3 and molecularly adsorbed NH_3 on Lewis acid sites, respectively. In comparison with bauxite, such bands in Cu/bauxite are slightly blue-shifted to 1250 cm^{-1} and red-shifted to 1624 cm^{-1}, respectively. The redshift is attributed to the weakening of Cu–NH_3 bond, while the blue shift corresponds to the strengthening of Cu–NH_3 bond.[31,32] For Ni/bauxite, only the latter band is red-shifed to 1622 cm^{-1}. Mn/bauxite shows two bands at 1236 and 1329 cm^{-1} owing to the coordination of NH_3 on Lewis acid sites. Other two bands at 1489 and 1438 cm^{-1} in bauxite may be assigned to -NH_2 vibration and anti-symmetric bending vibration of NH_4^+ ions on Brønsted acid sites, respectively.[33,34] In Mn/bauxite, the band at 1387 and 1498 cm^{-1} represent $-NH_2$ vibration on Brønsted acid sites. Additionally, the band at 1671 cm^{-1} indicates anti-symmetric bending vibration of NH_4^+ ions. It should be mentioned that Cu/bauxite and Ni/bauxite just show one peak of NH_4^+ at 1408 cm^{-1} and one peak of $-NH_2$ vibration on Brønsted acid sites at 1370 cm_{-1}, respectively.

In order to clarify correlation between SCR activity and acid sites in bauxite and M/bauxite, the amounts of Brønsted and Lewis acid

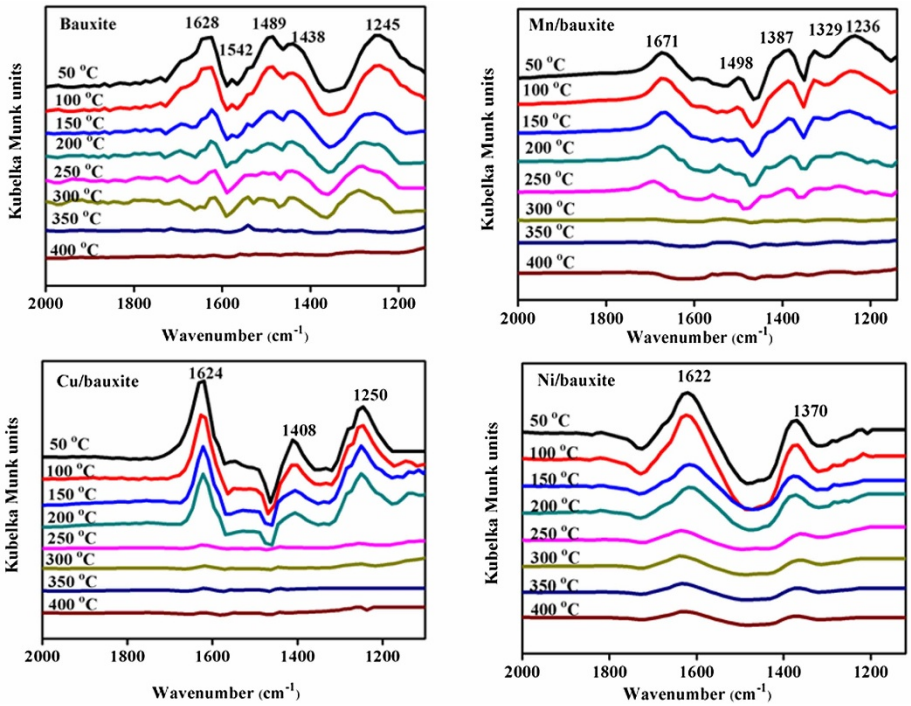

Figure 5 | ***in situ*** **DRIFTS of NH_3 adsorption in bauxite and M/bauxite.**

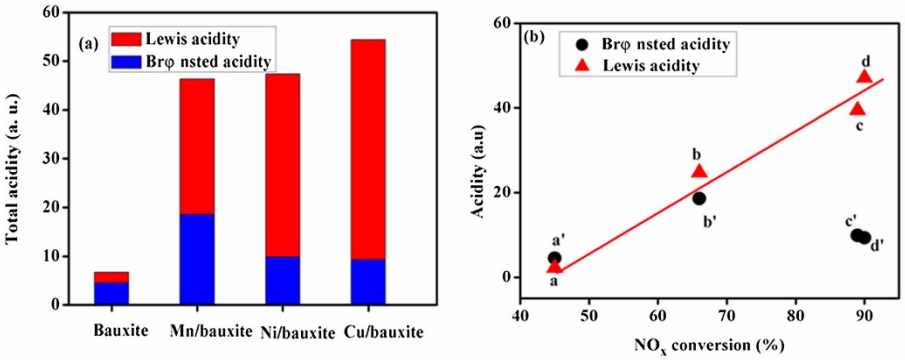

Figure 6 | (a) Lewis, Brønsted and total acid sites calculated based on *in situ* DRIFTS spectra; (b) The correlation of Lewis and Brønsted acidity versus NO_x conversion at 200 °C. *a*-bauxite; *b*-Mn/bauxite; *c*-Ni/bauxite and *d*-Cu/bauxite.

sites were calculated based on *in situ* DRIFTS at 200 ℃. As shown in Figure 6, the amount of Lewis acid sites is closely associated with SCR activity, while no such correlation is observed for Brønsted acid sites. The ratios of Lewis to Brønsted acid sites are in the order: Cu/bauxite (4.83) > Ni/bauxite (3.80) > Mn/bauxite (1.49) > bauxite (0.48) (Table S1). These results clearly indicate that Lewis acidity in M/bauxite is more important than Brønsted acidity for low-temperature SCR activity.

Discussion

In our work, a series of M/bauxite catalysts were presented for low-temperature and SO_2-tolerant SCR of NO_x, these catalysts are cheap, non-toxic and readily available. M and FeO_x in M/bauxite are confirmed to be main active species in SCR of NO_x. Interestingly, Cu/bauxite shows wide temperature window over 50–400 ℃ in SCR of NO_x. NO_x conversion is more than 80% at 50–200 ℃, which is more than two times than that in V_2O_5/TiO_2, while NO_x conversion at 300–400 ℃ reaches above 98%. N_2 selectivity at 50–400 ℃ is more than 98%. Moreover, Cu/bauxite exhibits strong resistance against SO_2 and good regenerability in SCR of NO_x, while V_2O_5/TiO_2 was greatly deactivated in the presence of SO_2. The superior SCR performances in Cu/bauxite are related to better low-temperature reducibility, larger desorption amounts of NO_x and NH_3 as well as more Lewis acidity amount. These results has showed Cu/bauxite is a promising SCR catalyst for low-temperature removal of NO_x, which provides further incentive for investigation of practical application in low-temperature NO_x abatement.

Methods

M/bauxite (M = Cu, Mn and Ni) were prepared by wet deposition method, and thermal-treatment natural bauxite was used a support.[21] Bauxite (1.0 g) in continuous stirring water (50 mL) was heated to 60 ℃ for 3 h, transition metal nitrates (3 wt% Cu, Mn and Ni) in H_2O (10 mL) were dropwisely added, the resultant mixture was evaporated to dryness at 60 ℃, dried at 120 ℃ overnight and calcined at 550 ℃ for 2 h. The obtained samples were denoted as M/bauxite (M = Cu, Mn and Ni). 3 wt% V_2O_5/TiO_2 was prepared according to the modified literature methods. [5]

XRD patterns were recorded on a RIGAKU-Miniflex II X-ray diffractometer with Cu K_α radiation (λ = 1.5406 Å). N_2 physisorption measurement was performed on an ASAP 2020 apparatus, the sample was degassed in vacuo at 180 ℃ at least 6 h before the measurement. XPS analysis was performed on Physical Electronics Quantum 2000, equipped with a monochromatic Al-K_α source (K_α = 1,486.6 eV) and a charge neutralizer; the catalysts were calcined at 400 ℃ before XPS test. The components of bauxite were determined using a PANalytical Axios XRF spectrometer with a rhodium tube as the source of radiation. The results were analyzed by IQ^+ and the concentrations were normalized to 100%. ICP analysis was performed on a JY Ultima2 spectrometer.

H_2-TPR was performed on AutoChem II 2920 equipped with a TCD detector. A sample of 0.1 g was pretreated in air flow (30 mL/min) at 500 ℃ for 0.5 h, and followed by purging with Ar (30 mL/min) for 0.5 h. After cooling to room temperature, the temperature was increased at 5 ℃/min up to 800 ℃ by a temperature-programmed controller in gas flow of 10 vol% H_2/Ar (30 mL/min). H_2-TPR was measured from 50 to 800 ℃ at 5 ℃/min.

NH_3-TPD was conducted on an AutoChem 2920 equipped with a TCD detector. A sample of 0.1 g was pretreated in Ar at 500 ℃ for 1 h. After cooled to 50 ℃, the sample was exposed to 5.01% NH_3/Ar for 30 min, followed by flushing with Ar at 100 ℃ to remove physisorbed ammonia, and then cooled down to 50 ℃. NH_3-TPD was measured from 50 to 800 ℃ in a N_2 flow at a rate of 10 ℃/min.

NO_x-TPD experiments was conducted on an AutoChem 2920 equipped with a TCD detector. A sample of 0.2 g was pretreated in 8 vol% O_2/Ar at 500 ℃ for 2 h with a flow rate of 100 mL/min. After cooled to room temperature, the sample was exposed to a mixture gas of 540 ppm NO and 8 vol% O_2/Ar balanced by N_2 (Total gas flow rate: 230 mL/min) until recovery of the inlet NO_x concentration, followed by flushing with 8 vol% O_2/Ar to remove weakly absorbed NO_x species until the disappearance of NO_x species in 8 vol% O_2/Ar stream. NO_x-TPD experiment was carried out from room temperature to 600 ℃ in a N_2 flow at a rate of 3 ℃/min. The outlet gas flow was continuously monitored using chemiluminescence NO-NO_2-NO_x detector.

in situ DRIFTS spectra were recorded on a Nicolet Nexus FT-IR spectrometer in the range of 650–4000 cm^{-1} with 32 scans at a resolution of 4 cm^{-1}. Prior to each experiment, the sample was pretreated at 350 ℃ for 0.5 h in a flow of N_2 to remove any adsorbed impurities, and then cooled down to 50 ℃. The background spectrum was collected in N_2 and automatically subtracted from the sample spectra. Afterward, NH_3 (500 ppm balanced with He) was introduced to the cell with gas flow rate of 30 mL/min at 100 ℃ for 1 h to ensure complete absorption saturation. Physisorbed ammonia was removed by flushing wafer with helium at 100 ℃ for 3 h. DRIFTS spectra were recorded by evacuation of ammonia at successive temperatures from 50 to 400 ℃.

SCR activity measurement was performed in a fixed-bed stainless steel reactor (inner diameter = 8 mm), and a thermocouple was inserted in the center of catalyst bed to measure test temperature. Before each test, a 0.5 g of 20–30 mesh sample was reduced by 5 vol% H_2/Ar at 500 ℃ for 2 h, and followed by treatment using 3 vol% O_2/Ar at 500 ℃ for 2 h. NH_3 adsorption experiment was carried out in the temperature range of 50–200 ℃ using 500 ppm of NH_3 and 2 vol% O_2 balanced by Ar. At test temperature, the catalysts were placed in the reactor until outlet NO gas reached the expected equilibrium concentration, in order to ensure that the decrement of NO concentration was caused by SCR instead of the adsorption by the catalysts. The feed gas (540 ppm NO, 500 ppm NH_3, 0.67 vol% H_2 and 3 vol% O_2 balanced by N_2) was introduced using mass-flow controllers at a total flow rate of 600 mL/min, and the corresponding GHSV is 72, 000 h^{-1}. The outlet gas concentrations were collected until a steady state was achieved at the given temperature for 1 h. H_2O resistance was examined by introducing 10 vol% H_2O into feed gas at 200 ℃. SO_2 poisoning experiment was performed by exposing samples to feed gas containing additional 100 ppm SO_2 at 350 ℃. The sulfated samples were regenerated by 3.5 vol% H_2 at 500 ℃ for 60 min. The outlet NO_x concentration was measured using on-line chemiluminescence NO-NO_2-NO_x analyzer (model 42i-HL, Thermo Scientific). The outlet N_2O was analyzed using an FTIR spectrometer (Nicolet Nexus 6700) with a heated, multiple-path gas cell. The N_2 selectivity was analyzed using a GC7820 A. NO_x conversion under steady-state conditions for 1 h was calculated according to the following equation.

$$NO_x \text{ conversion } (\%) = (NO_{x\,\text{inlet}} - NO_{x\,\text{outlet}})/NO_{x\,\text{inlet}} \times 100\%$$

Transient response method (TRM) of Cu/bauxite was carried out at 150 ℃ according to literature methods.[7] Before each test, a 0.1 g sample was pretreated in air flow (30 mL/min) at 500 ℃ for 0.5 h. After cooling to 150 ℃, 500 ppm NO was introduced and the reactor was maintained at steady state for 30 min, then a feed gas of 500 ppm NO, 0.05 vol% O_2 and 1 vol% H_2 and 500 ppm NH_3 balanced by Ar were introduced in the next step. The outlet gas concentrations were continuously monitored by a mass spectrometer and UV analyzer.

1. Forzatti, P.; Nova, I. & Tronconi, E. Enhanced NH_3 Selective Catalytic Reduction for NO_x Abatement. *Angew. Chem. Int. Ed.* **48**, 8366–8368 (2009).
2. Peng, Y., *et al.* Catalysis for NOx Abatement *Appl. Energy* **86**, 2283–2297 (2009).

3. Huang, H. Y.; Long, R. Q. & Yang, R. T. A highly sulfur resistant Pt-Rh/TiO_2/Al_2O_3 storage catalyst for NO_x reduction under lean-rich cycles. *Appl. Catal. B: Environ.* **33**, 127–136(2001).
4. Grossale, A.; Nova, I.; Tronconi, E.; Chatterjee, D. & Weibel. M. The Chemistry of the NO/NO2–NH3 "fast" SCR Reaction over Fe-ZSM5 Investigated by Transient Reaction Analysis. *J. Catal.* **256**, 312–322 (2008).
5. Mihai, O., *et al*. The Effect of Cu-loading on Different Reactions Involved in NH3-SCR over Cu-BEA Catalysts. *J. Catal.* **311**, 170–181 (2014).
6. Thirupathi, B. & Smirniotis, P. G. Co-doping a Metal (Cr, Fe, Co, Ni, Cu, Zn, Ce, and Zr) on Mn/TiO_2 Catalyst and its Effect on the Selective Reduction of NO with NH_3 at Low-Temperatures. *Appl. Catal. B: Environ.* **110**, 195–206 (2011).
7. Thirupathi, B. & Smirniotis, P. G. Nicked-doped Mn/TiO_2 as an Efficient Catalyst for the Low-Temperature SCR of NO with NH_3: Catalytic Evalauation and Characterizations. *J. Catal.* **288**, 74–83(2012).
8. Chen, L.; Li, J. & Ge, M. The Poisoning Effect of Alkali Metals doping over Nano V_2O_5-WO_3/TiO_2 Catalysts on Selective Catalytic Reduction of NO_x by NH_3. *Chem. Eng. J.* **170**, 531–537 (2011).
9. Topsoe, N. Y. Mechanism of the Selective Catalytic Reduction of Nitric Oxide by Ammonia Elucidated by in Situ On-Line Fourier Transform Infrared Spectroscopy. *Science* **265**, 1217–1219 (1994).
10. Chen, L.; Li, J. & Ge, M. Promotional Effect of Ce-doped V_2O_5-WO_3/TiO_2 with Low Vanadium Loadings for Selective Catalytic Reduction of NO_x by NH_3. *J. Phys. Chem. C* **113**, 21177–21184 (2009).
11. Peng, Y.; Wang, C. & Li, J. Structure-activity Relationship of VO_x/CeO_2 Nanorod for NO Removal with Ammonia. *Appl. Catal. B: Environ.* **144**, 538–546 (2014).
12. Peng, Y.; Qu, R.; Zhang, X. & Li, J. The Relationship between Structure and Activity of MoO_3-CeO_2 Catalysts for NO removal: Influences of Acidity and Reducibility. *Chem. Commun.* **49**, 6215–6217 (2013).
13. Colombo,M.; Nova, I. & Tronconi. E. NO2 Adsorption on Fe- and Cu-zeolite Catalysts: The Effect of the Catalyst Redox State. *Appl. Catal. B: Environ.* **111–112**, 433–444 (2012).
14. Paredis, K., *et al*. Evolution of the Structure and Chemical State of Pd Nanoparticles during the in Situ Catalytic Reduction of NO with H_2. *J. Am. Chem. Soc.* **133**, 13455–13464 (2011).
15. Smirniotis, P. G.; Peña, D. A. & Uphade, B. S. Low-Temperature Selective Catalytic Reduction (SCR) of NO with NH_3 by Using Mn, Cr, and Cu Oxides Supported on Hombikat TiO_2. *Angew. Chem. Int. Ed.* **40**, 2479–2482 (2001).
16. Liu, F. D.; He, H. & Xie, L. J. on the Specific Deoxidation Behavior of Iron Titanate Catalyst for the Selective Catalytic Reduction of NO_x with NH_3. *ChemCatChem* **5**, 3760–3769 (2013).
17. Liu, Z.; Zhu, J.; Li, J.; Ma, L. & Woo, S. I. Novel Mn-Ce-Ti Mixed-Oxide Catalyst for the Selective Catalytic Reduction of $NO_x$with NH_3. *ACS Appl. Mater. Interfaces.* **6**, 14500–14508 (2014).
18. Wan, Y., *et al*. Ni-Mn bi-metal Oxide Catalysts for the Low Temperature SCR Removal of NO with NH_3. *Appl. Catal. B: Environ.* **148–149**, 114–122 (2014).
19. Wang, W., *et al*. Mixed-Phase Oxide Catalyst Based on Mn-Mullite (Sm, Gd)Mn_2O_5 for NO Oxidation in Diesel Exhaust. *Science* **337**, 832–835 (2012).
20. Royer, S., *et al*. Perovskites as Substitutes of Noble Metals for Heterogeneous Catalysis: Dream or Reality, *Chem. Rev.* **114**, 10292–10368 (2014).
21. Jiang, L. L.; Ye, B. H. & Wei, K. M. Effects of CeO_2 on Structure and Properties of Ni-Mn-K/bauxite Catalysts for Water-gas Shift Reaction. *J. Rare Earth* **26**, 352–356 (2008).
22. Wang, X. Y.; Chen, Z. L.; Luo, Y. J.; Jiang, L. L. & Wang, R. H. Cu/Ba/bauxite: an Inexpensive and Efficient Alternative for Pt/Ba/Al_2O_3 in NO_x Removal. *Sci. Rep.* **3**, 1559 (2013).
23. Wang, X. Y.; Jiang, L. L.; Wang, J. Y. & Wang, R. H. Ag/bauxite Catalysts: Improved Low-temperature Activity and SO_2 Tolerance for H_2-promoted NH_3-SCR of NO_x. *Appl. Catal. B: Environ.* **165**, 700–705 (2015).
24. Ordóñez, S.; Sastre, H. & Díez, F. V. Characterisation and Deactivation Studies of Sulfided Red Mud used as Catalyst for the Hydrodechlorination of Tetrachloroethylene *Appl. Catal. B: Environ.* **29**, 263–273(2001).
25. Suárez, S.; Martín, J. A.; Yates, M.; Avila, P. & Blanco, J. N_2O Formation in the Selective Catalytic Reduction of NO_x with NH_3 at Low Temperature on CuO-supported Monolithic Catalysts. *J. Catal.* **229**, 227–236 (2005).
26. Yao, X., *et al*. Tailoring Copper Valence States in CuO_δ/γ-Al_2O_3 Catalysts by an in situ Technique Induced Superior Catalytic Performance for Simultaneous Elimination of NO and CO. *Phys. Chem. Chem. Phys.* **15**, 14945–14950 (2013).
27. Moreno-Tost, R.; Santamaría-González, J.; Maireles-Torres, P.; Rodríguez-Castellón, E. & Jiménez-López, A. Nickel Oxide Supported on Zirconium-doped Mesoporous Silica for Selective Catalytic Reduction of NO with NH_3. *J. Mater. Chem.* **12**, 3331–3336 (2002).
28. Shen, Y. & Zhu, S. Deactivation Mechanism of Potassium Additives on $Ti_{0.8}Zr_{0.2}Ce_{0.2}O_{2.4}$ for NH_3-SCR of NO. *Catal. Sci. Technol.* **2**, 1806–1810(2012).
29. Chmielarz, L., *et al*. SCR of NO by NH_3 on Alumina or Titania Pillared Montmorillonite Modified with Cu or Co Part II. Temperature programmed Studies. *Appl. Catal. B: Environ.* **53**, 47–61 (2004).
30. Zhang, D., *et al*. In situ Supported MnO_x-CeO_x on Carbon Nanotubes for the Low-temperature Selective Catalytic Reduction of NO with NH_3. *Nanoscale* **5**, 1127–1136 (2013).
31. Shan, W.; Liu, F.; He, H.; Shi, X. & Zhang, C. A Superior Ce-W-Ti Mixed Oxide Catalyst for the Selective Catalytic Reduction of NO_x with NH_3. *Appl. Catal. B: Environ.* **115**, 100–106 (2012).
32. Wang, D.; Zhang, L.; Kamasamudram, K. & Epling, W. S. In Situ-DRIFTS Study of Selective Catalytic Reduction of NO_x by NH_3 over Cu-Exchanged SAPO-34. *ACS Catal.* **3**, 871–881(2013).
33. Chen, L.; Li, J. & Ge, M. DRIFT Study on Cerium-Tungsten/Titiania Catalyst for Selective Catalytic Reduction of NO_x with NH_3. *Environ. Sci. Technol.* **44**, 9590–9596 (2010).
34. Yang, X., *et al*. DRIFTS Study of Ammonia Activation over CaO and Sulfated CaO for NO Reduction by NH_3. *Environ. Sci. Technol.* **45**, 1147–1151 (2011).

Acknowledgments

This work was financially supported by 973 Program (2011CBA00502, 2013933202), Major Project of Fujian Province (2013H0061) and "One Hundred Talent Project" of Chinese Academy of Sciences.

Author contribution

X.W. and W.W. prepared the sample; X.W. and R.W. designed the experiments and wrote the paper. X.W., Z C. and W.W. performed the measurements and analyzed the data. All authors discussed the results and commented on the manuscript.

Additional information

Supplementary information accompanies this paper at http://www.nature.com/scientificreports;

Competing financial interests: The authors declare no competing financial interests.

How to cite this article: Wang, X. *et al.* Bauxite-supported Transition Metal Oxides: Promising Low-temperature and SO_2-tolerant Catalysts for Selective Catalytic Reduction of NO_x. *Sci. Rep.* **5**, 9766; DOI:10.1038/srep09766 (2015).